LONGITUDINAL CYTOKINE DYNAMICS DURING PALATAL WOUND HEALING AFTER FREE GINGIVAL GRAFT: A COMPARATIVE ANALYSIS OF STELLALIFE, CHLORHEXIDINE, AND CONTROL

Veronica Xia, Amber Kreko, Eswar Kandaswamy, Panagiotis Dragonas, Vinayak Joshi
Louisiana State University School of Dentistry, New Orleans, LA

ABSTRACT

Background: Free gingival grafting (FGG) generates a palatal donor site that heals by secondary intention, producing a dynamic inflammatory microenvironment. StellaLife is a botanical-based adjunctive rinse with proposed anti-inflammatory properties; however, its in vivo effects on cytokine expression remain unclear.
Objective: To characterize temporal cytokine dynamics during palatal wound healing and compare profiles among StellaLife (SL), chlorhexidine (CHX), and saline control.
Methods: Twenty-seven subjects undergoing FGG were randomized to SL, CHX, or saline. Wound exudate was collected at Days 0, 7, 14, 21, and 28; only Days 7–21 yielded quantifiable results. Ten cytokines (IL-8, IL-10, EGF, VEGF-A, MMP-8, IL-1β, TIMP-1, MPO, PDGF-BB, IL-17) were analyzed using Luminex MAGPIX.
Results: Three of ten cytokines were excluded due to being outside of detection limits. The remaining seven cytokines demonstrated significant reductions over time ($p < 0.01$), with peak levels at Day 7 and near resolution by Day 21. No significant intergroup differences were observed at any time point or in longitudinal change analyses ($p > 0.05$).
Conclusions: Palatal wound healing following FGG is characterized by a coordinated, time-dependent reduction in inflammatory mediators driven primarily by intrinsic biological processes rather than adjunctive therapies.

INTRODUCTION

Background and Significance

Free gingival grafting (FGG) is a foundational technique in periodontal plastic surgery used to increase the zone of keratinized and attached gingiva around teeth and implants.[1] The procedure involves harvesting full-thickness epithelial–connective tissue from the hard palate, thereby creating a donor site that heals entirely by secondary intention.[2]

Secondary intention healing is a highly coordinated biological process consisting of four overlapping phases: (1) hemostasis, characterized by fibrin clot formation; (2) inflammation, involving neutrophil and macrophage recruitment with subsequent cytokine and chemokine release; (3) proliferation, marked by fibroblast activity, collagen synthesis, and re-epithelialization; and (4) tissue maturation and remodeling, involving extracellular matrix reorganization.[3,4] Although predictable, this process is associated with significant postoperative morbidity, including pain and delayed healing, thereby prompting investigation into adjunctive therapeutic strategies aimed at improving patient outcomes.[2]

StellaLife VEGA Oral Care Recovery Kit

StellaLife VEGA Oral Care Recovery Kit is a novel, opioid-free, homeopathic rinse and gel system introduced as a postoperative adjunct in oral surgery.[5] The formulation contains 16 active botanical components, including *Arnica montana*, *Calendula officinalis*, *Chamomilla*, *Echinacea angustifolia*, *Plantago major*, and *Azadirachta indica* (neem), which have been individually associated with anti-inflammatory and wound-healing properties.

Preclinical and clinical evidence suggests potential therapeutic benefits of this formulation. Lee and Suzuki reported reduced postoperative pain and decreased opioid reliance following block bone graft procedures in patients using StellaLife.[7] In vitro studies have demonstrated that *Arnica montana* extract can reduce pro-inflammatory cytokines such as TNF-α, IL-1, and IL-6,[8] while *Plantago major* has shown dose-dependent acceleration of wound closure.[9] Furthermore, Fujioka-Kobayashi et al. demonstrated that StellaLife-treated gingival fibroblasts exhibit greater viability, preserved migration capacity, and reduced expression of pro-inflammatory cytokines compared with cells exposed to chlorhexidine (CHX).[6]

Chlorhexidine as the Reference Standard

Chlorhexidine gluconate (0.12%) remains the gold standard antimicrobial rinse following periodontal surgery.[11] Its effectiveness is attributed to broad-spectrum antibacterial activity; however, it has been associated with cytotoxic effects on gingival fibroblasts, including dose-dependent reductions in collagen synthesis and cellular viability.[10,11] Clinically, CHX use is also associated with adverse effects such as tooth staining, taste alteration, and mucosal sloughing.[16]

Despite these concerns, recent clinical evidence suggests that these in vitro cytotoxic effects may not translate into impaired healing outcomes in vivo. Notably, Pardo et al. (2024) demonstrated that early periodontal wound healing in CHX-treated patients was not inferior to that observed in control groups in a randomized controlled trial.[12]

Inflammatory Mediators in Wound Healing

Inflammatory mediators play a central role in regulating wound healing dynamics. Ten cytokines and growth factors were initially selected for analysis based on their established roles in inflammation, tissue repair, and remodeling.[13,14,15]

IL-8 functions as an early neutrophil chemoattractant, while IL-1β acts as a key macrophage-derived cytokine amplifying the inflammatory cascade. In contrast, IL-10 serves as an anti-inflammatory mediator facilitating resolution of inflammation. Epidermal growth factor (EGF) promotes epithelial proliferation and re-epithelialization, whereas vascular endothelial growth factor A (VEGF-A) supports angiogenesis. Matrix metalloproteinase-8 (MMP-8), a neutrophil-derived collagenase, mediates extracellular matrix remodeling, and its activity is regulated by tissue inhibitor of metalloproteinases-1 (TIMP-1).

Additional mediators, including platelet-derived growth factor-BB (PDGF-BB), interleukin-17 (IL-17), and myeloperoxidase (MPO), contribute to fibroblast recruitment, inflammatory signaling, and neutrophil activation, respectively, further underscoring the complexity of the wound-healing microenvironment.

Rationale and Hypothesis

Despite increasing clinical use of adjunctive rinses such as StellaLife, there remains limited in vivo evidence evaluating their effects on the biochemical wound-healing environment. To date, no studies have directly characterized cytokine dynamics in palatal wound exudate following FGG in response to commonly used postoperative rinses.

Therefore, the aim of this study was to determine whether StellaLife alters the inflammatory cytokine profile during palatal wound healing compared with chlorhexidine and saline control.

Hypothesis: The use of StellaLife will result in altered inflammatory mediator expression at the palatal donor site following FGG compared with chlorhexidine and saline.

Specific Aims

- To characterize the longitudinal temporal changes of seven inflammatory mediators (IL-8, IL-10, EGF, VEGF-A, MMP-8, IL-1β, and TIMP-1) in palatal wound exudate over the healing period.
- To compare inflammatory mediator profiles among StellaLife, chlorhexidine, and saline control groups at Days 0, 7, 14, 21, and 28.
- To evaluate the inter-cytokine correlation structure of the wound exudate mediator panel and its relationship to healing time. This aim was included as an exploratory analysis to characterize the network-level coordination of the inflammatory response.

MATERIALS AND METHODS

Study Design and Participant Selection

This study was designed as a prospective, randomized, controlled clinical trial conducted at the Louisiana State University School of Dentistry (LSUSD) Postgraduate Periodontics Clinic. The study protocol was approved by the Institutional Review Board, and all participants provided informed consent prior to enrollment.

A total of 30 subjects requiring free gingival grafting (FGG) procedures were recruited. Inclusion criteria included individuals aged 21–48 years, with no medications affecting periodontal status within the preceding six months, no known allergies to study products, non-smoking status, absence of pregnancy or lactation, and adequate oral hygiene. Exclusion criteria included prior surgery within four months, harvesting from previously treated donor sites, and systemic conditions known to impair wound healing.

Randomization and Treatment Protocol

Participants were randomly assigned using a computer-generated allocation sequence with concealed assignment into one of three groups:

(1) saline control,

(2) 0.12% chlorhexidine (CHX) rinse with placebo gel, or

(3) StellaLife VEGA rinse and gel.

All subjects initiated their assigned regimen on the day of surgery and continued twice daily throughout the study period. Standardized FGG procedures were performed for all participants. A palatal stent was used to standardize donor site dimensions (6 × 15 mm), and a vacuum-formed copyplast stent was provided for postoperative protection.

Sample Collection

Palatal wound exudate samples were collected at Days 0, 7, 14, 21, and 28 postoperatively. Sterile absorbent paper points (size 40) were placed at the donor site for 30 seconds and transferred into cryovials containing phosphate-buffered saline (PBS). Samples were stored at −40°C until analysis. Due to assay detection limitations, only samples obtained at Days 7, 14, and 21 yielded reliably quantifiable cytokine concentrations and were included in the final analysis.

Luminex MAGPIX Multiplex Immunoassay

Cytokine quantification was performed using the Luminex MAGPIX multiplex immunoassay platform, which enables simultaneous detection of multiple analytes from small sample volumes. The initial panel included ten mediators based on their roles in wound healing biology (13–15): IL-8, IL-10, EGF, VEGF-A, MMP-8, IL-1β, TIMP-1, PDGF-BB, MPO, and IL-17. PDGF-BB and IL-17 were below detection limits, while MPO exceeded the upper limit; these were excluded. The final analytical panel included IL-8, IL-10, EGF, VEGF-A, MMP-8, IL-1β, and TIMP-1.

Statistical Analysis

Data distribution was assessed using the Shapiro–Wilk test, confirming non-normal distributions. Nonparametric methods were therefore used. Descriptive statistics were reported as median and interquartile range (IQR). Kruskal–Wallis testing was used for group and time comparisons, followed by Dunn–Bonferroni post hoc testing. Change scores were calculated relative to Day 7, representing peak inflammatory activity. Spearman correlation coefficients were used to evaluate cytokine relationships and time-dependent trends. Statistical significance was set at $\alpha = 0.05$.
Due to sample size limitations, findings should be interpreted as exploratory.

RESULTS

Study Population

Twenty-seven subjects contributed wound exudate samples: Control (n = 8), CHX (n = 10), and StellaLife (n = 9) at Day 7, with one StellaLife subject absent at Day 21 (n = 8). Demographics: ages 21–48 years; 15 male (56%), 12 female (44%).

Excluded Analytes

Three of ten Luminex MAGPIX analytes were excluded from final analysis due to concentrations outside assay detection limits: PDGF-BB (below the lower detection limit), IL-17 (below the lower detection limit), and MPO (above the upper detection limit). The remaining seven analytes demonstrated reliably quantifiable concentrations and constitute the final analytical panel.

Descriptive Statistics

Table 1 presents descriptive statistics for all seven analytes by group and time point. All analytes demonstrated markedly elevated concentrations at Day 7, with substantial reduction by Day 14 and further resolution approaching the detection floor by Day 21. These patterns were consistent across all treatment groups and analytes.

Table 1. Descriptive statistics of analyte concentrations by group and time point (Median [IQR], Min–Max; all values in pg/mL).

Analyte	Group	Day	Median (IQR) pg/mL	Range (Min–Max) pg/mL	n
IL-8	Control	7	534.19 (121.06–704.28)	99.59–1503.00	8
IL-8	Control	14	22.34 (5.33–32.65)	1.37–138.18	8
IL-8	Control	21	1.37 (1.37–1.94)	1.37–5.09	8
IL-8	CHX	7	114.93 (41.47–242.89)	14.77–1503.00	10
IL-8	CHX	14	1.37 (1.37–4.46)	1.37–78.72	10
IL-8	CHX	21	1.37 (1.37–1.37)	1.37–3.41	10
IL-8	StellaLife	7	153.69 (35.39–304.01)	3.04–1503.00	9

Analyte	Group	Day	Median (IQR) pg/mL	Range (Min–Max) pg/mL	n
IL-8	StellaLife	14	3.41 (1.37–128.11)	1.37–386.59	9
IL-8	StellaLife	21	1.37 (1.37–1.37)	1.37–46.66	8
IL-10	Control	7	9.15 (5.81–11.42)	2.23–13.92	8
IL-10	Control	14	2.23 (2.23–2.83)	2.23–15.50	8
IL-10	Control	21	2.23 (2.23–2.23)	2.23–2.23	8
IL-10	CHX	7	4.50 (2.23–8.04)	2.23–19.18	10
IL-10	CHX	14	2.23 (2.23–2.23)	2.23–8.76	10
IL-10	CHX	21	2.23 (2.23–2.23)	2.23–2.23	10
IL-10	StellaLife	7	6.52 (2.23–7.01)	2.23–13.66	9
IL-10	StellaLife	14	2.23 (2.23–7.76)	2.23–10.17	9
IL-10	StellaLife	21	2.23 (2.23–2.23)	2.23–2.23	8
EGF	Control	7	94.09 (61.62–134.45)	23.24–151.20	8
EGF	Control	14	27.13 (6.11–39.30)	3.28–193.95	8
EGF	Control	21	3.28 (3.28–3.28)	3.28–9.81	8
EGF	CHX	7	51.45 (16.78–90.44)	3.28–166.68	10
EGF	CHX	14	3.28 (3.28–3.28)	3.28–92.42	10
EGF	CHX	21	3.28 (3.28–3.28)	3.28–3.28	10
EGF	StellaLife	7	56.68 (12.00–75.06)	3.28–142.24	9
EGF	StellaLife	14	3.28 (3.28–80.44)	3.28–142.53	9
EGF	StellaLife	21	3.28 (3.28–3.28)	3.28–19.35	8
VEGF-A	Control	7	60.27 (42.01–77.00)	16.80–101.03	8
VEGF-A	Control	14	11.27 (5.74–19.37)	5.74–105.42	8
VEGF-A	Control	21	5.74 (5.74–5.74)	5.74–11.49	8
VEGF-A	CHX	7	32.40 (15.05–60.83)	5.74–579.89	10
VEGF-A	CHX	14	5.74 (5.74–5.74)	5.74–68.33	10
VEGF-A	CHX	21	5.74 (5.74–5.74)	5.74–5.74	10
VEGF-A	StellaLife	7	29.37 (5.74–51.16)	5.74–246.34	9
VEGF-A	StellaLife	14	5.74 (5.74–53.29)	5.74–139.51	9
VEGF-A	StellaLife	21	5.74 (5.74–5.74)	5.74–13.21	8
MMP-8	Control	7	46,377 (23,882–78,619)	8,890–78,619	8

Analyte	Group	Day	Median (IQR) pg/mL	Range (Min–Max) pg/mL	n
MMP-8	Control	14	8,706 (2,816–13,349)	115–78,619	8
MMP-8	Control	21	115 (115–434)	115–1,977	8
MMP-8	CHX	7	17,564 (5,725–42,278)	1,514–78,619	10
MMP-8	CHX	14	115 (115–1,602)	115–41,192	10
MMP-8	CHX	21	115 (115–115)	115–115	10
MMP-8	StellaLife	7	20,755 (4,824–32,462)	655–78,619	9
MMP-8	StellaLife	14	1,953 (297–26,839)	115–43,393	9
MMP-8	StellaLife	21	115 (115–115)	115–6,359	8
IL-1β	Control	7	260.28 (144.80–491.43)	59.72–1,769	8
IL-1β	Control	14	26.72 (18.18–34.60)	4.07–100.63	8
IL-1β	Control	21	4.07 (4.07–5.24)	4.07–20.13	8
IL-1β	CHX	7	114.06 (63.88–166.04)	22.92–3,384	10
IL-1β	CHX	14	4.07 (4.07–14.25)	4.07–70.48	10
IL-1β	CHX	21	4.07 (4.07–4.07)	4.07–4.07	10
IL-1β	StellaLife	7	85.11 (33.39–203.84)	4.07–1,855	9
IL-1β	StellaLife	14	12.94 (4.07–44.07)	4.07–349.15	9
IL-1β	StellaLife	21	4.07 (4.07–4.07)	4.07–41.15	8
TIMP-1	Control	7	572.12 (249.83–725.65)	164.32–1,262	8
TIMP-1	Control	14	94.59 (61.02–258.13)	11.53–586.70	8
TIMP-1	Control	21	19.20 (11.53–40.00)	11.53–284.03	8
TIMP-1	CHX	7	418.03 (173.47–447.42)	51.06–2,753	10
TIMP-1	CHX	14	11.53 (11.53–43.29)	11.53–277.20	10
TIMP-1	CHX	21	11.53 (11.53–11.53)	11.53–33.22	10
TIMP-1	StellaLife	7	363.80 (173.40–505.75)	32.17–1,840	9
TIMP-1	StellaLife	14	79.67 (27.93–476.51)	11.53–3,854	9
TIMP-1	StellaLife	21	11.53 (11.53–15.36)	11.53–163.62	8

Within-Group Temporal Analysis

Kruskal-Wallis testing confirmed statistically significant time-dependent variation for all analytes within each group (Table 2; $p < 0.05$ for all, majority achieving $p < 0.01$). Dunn-Bonferroni post-hoc analysis confirmed that Day 7 concentrations were significantly higher than Day 21 for all analytes across all groups (adjusted $p < 0.05$). Comparisons between Days 14 and 21 were generally not significant, indicating the major inflammatory decline occurs within the first two weeks post-FGG.

Table 2. Kruskal–Wallis test results for time-dependent variation within each treatment group.

Analyte	Group	Kruskal-Wallis p-value (across time points)
IL-8	Control	9.78×10^{-5}
IL-8	CHX	3.70×10^{-5}
IL-8	StellaLife	2.53×10^{-3}
IL-10	Control	8.48×10^{-3}
IL-10	CHX	3.53×10^{-2}
IL-10	StellaLife	3.04×10^{-2}
EGF	Control	6.84×10^{-4}
EGF	CHX	2.86×10^{-4}
EGF	StellaLife	3.31×10^{-2}
VEGF-A	Control	1.31×10^{-3}
VEGF-A	CHX	1.27×10^{-3}
VEGF-A	StellaLife	5.49×10^{-2}
MMP-8	Control	3.76×10^{-4}
MMP-8	CHX	8.75×10^{-5}
MMP-8	StellaLife	2.23×10^{-3}
IL-1β	Control	9.56×10^{-5}
IL-1β	CHX	1.72×10^{-5}
IL-1β	StellaLife	6.79×10^{-3}
TIMP-1	Control	1.41×10^{-3}
TIMP-1	CHX	4.47×10^{-5}
TIMP-1	StellaLife	3.26×10^{-3}

Figure 1 presents boxplot distributions of all seven analytes pooled across treatment groups at each time point.

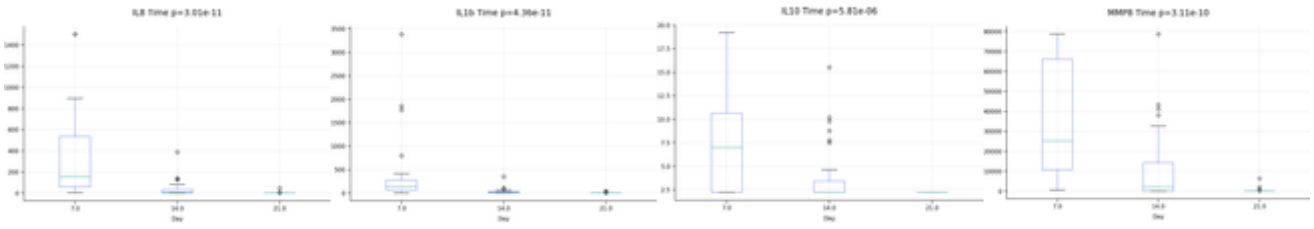

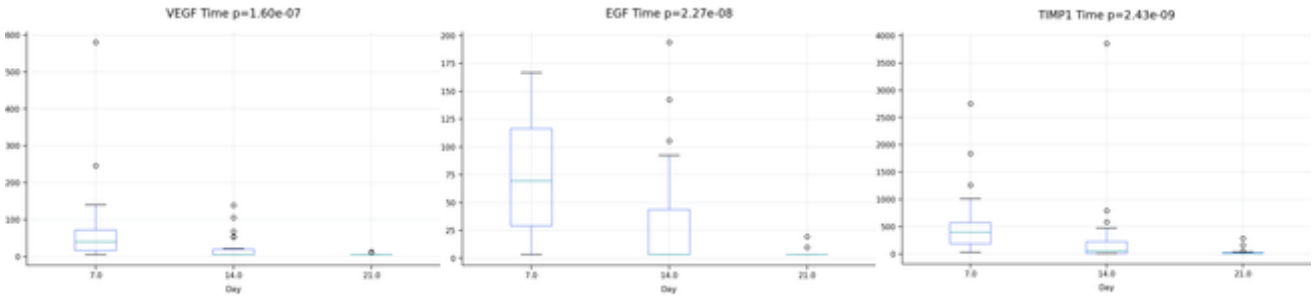

Figure 1. Pooled concentration of all seven inflammatory mediators at Days 7, 14, and 21 (all groups combined). Rows left→right: IL-8, IL-1β, IL-10, MMP-8 (top); VEGF-A, EGF, TIMP-1 (bottom). X-axis: Day; Y-axis: Concentration (pg/mL). Kruskal-Wallis p-values shown in individual panel titles.

Between-Group Comparisons

Kruskal–Wallis testing revealed no statistically significant differences in cytokine concentrations between treatment groups at any time point (Table 3; all $p > 0.05$). Across all analyses, cytokine expression followed a consistent temporal trajectory independent of treatment group. P-values ranged from 0.108 (TIMP-1) to 0.614 (IL-10). Figure 2 presents group comparison boxplots for all seven analytes with data pooled across time points.

Table 3. Between-group Kruskal-Wallis comparison (Control vs. CHX vs. StellaLife, all time points pooled).

Analyte	p-value (Control vs. CHX vs. StellaLife)
IL-8	0.273
IL-1β	0.322
IL-10	0.614
EGF	0.246
VEGF-A	0.459
MMP-8	0.152
TIMP-1	0.108

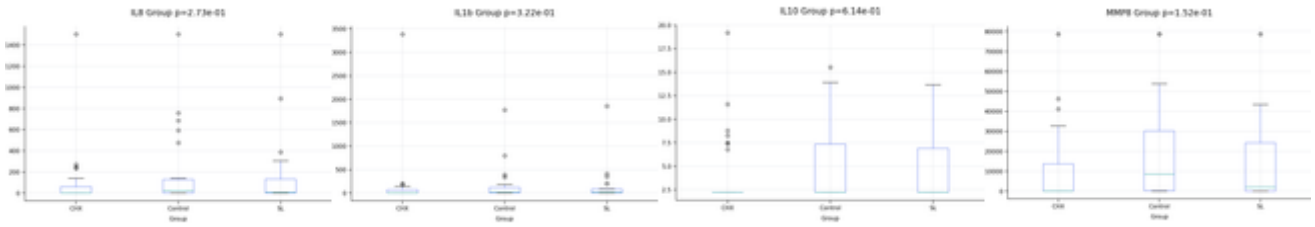

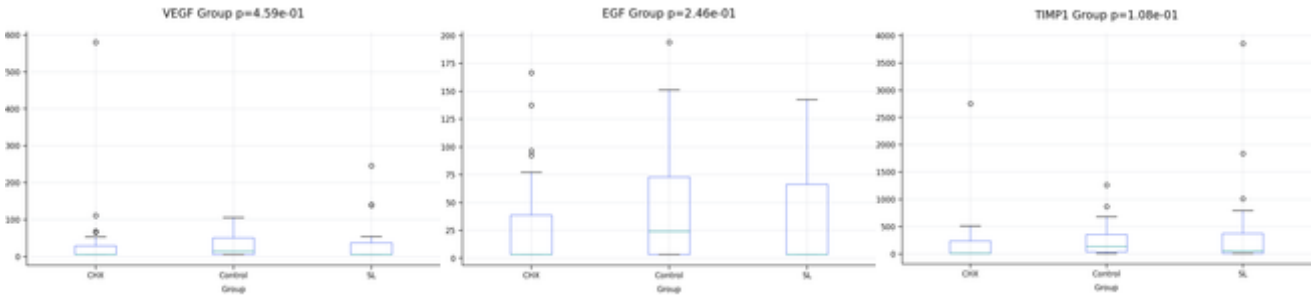

Figure 2. Group comparison boxplots — data pooled across Days 7, 14, and 21. Rows left→right: IL-8, IL-1β, IL-10, MMP-8 (top); VEGF-A, EGF, TIMP-1 (bottom). X-axis: Treatment group (CHX, Control, StellaLife); Y-axis: Concentration (pg/mL). All Kruskal-Wallis p-values > 0.05.

Longitudinal Trajectory Analysis

Longitudinal trajectory plots demonstrated consistent, parallel declining trajectories for all three treatment groups across all seven analytes (Figure 3). Change score analysis (Δ Day 21 − Day 7) confirmed that the magnitude of cytokine reduction did not differ significantly between groups for any analyte (Table 4; all $p > 0.05$). Figure 4 presents change score boxplot distributions. Across all analyses, cytokine expression followed a consistent temporal trajectory independent of treatment group.

Table 4. Change score between-group comparisons (Kruskal-Wallis).

Analyte	Change Score	p-value (between groups)
IL-8	Day 14−7	0.379
IL-8	Day 21−7	0.121
IL-1β	Day 14−7	0.443
IL-1β	Day 21−7	0.189
IL-10	Day 14−7	0.439
IL-10	Day 21−7	0.338
EGF	Day 14−7	0.238
EGF	Day 21−7	0.199
VEGF-A	Day 14−7	0.647
VEGF-A	Day 21−7	0.265
MMP-8	Day 14−7	0.425
MMP-8	Day 21−7	0.227
TIMP-1	Day 14−7	0.328
TIMP-1	Day 21−7	0.372

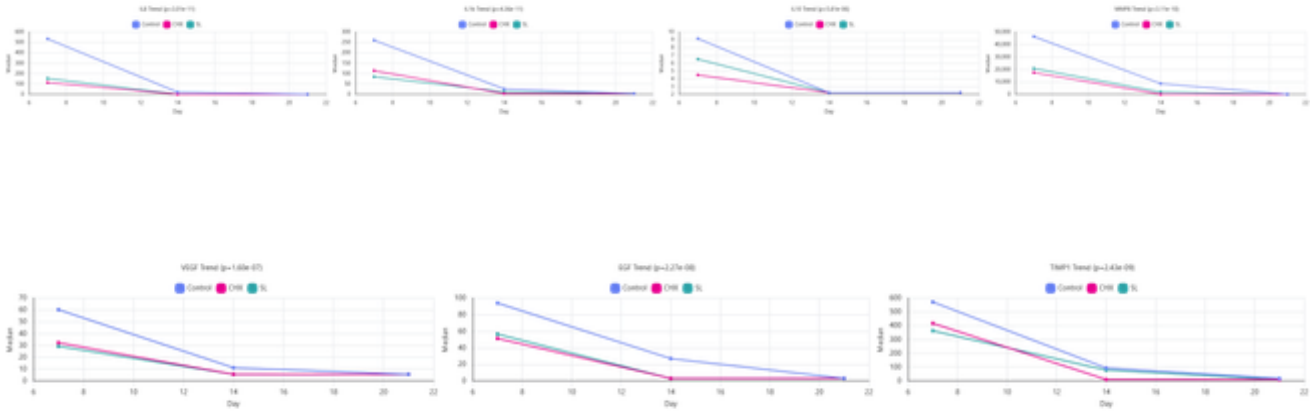

Figure 3. Longitudinal trajectory of median concentration by treatment group. Rows left→right: IL-8, IL-1β, IL-10, MMP-8 (top); VEGF-A, EGF, TIMP-1 (bottom). X-axis: Day (7, 14, 21); Y-axis: Median concentration (pg/mL). Blue = Control, Pink = CHX, Teal = StellaLife.

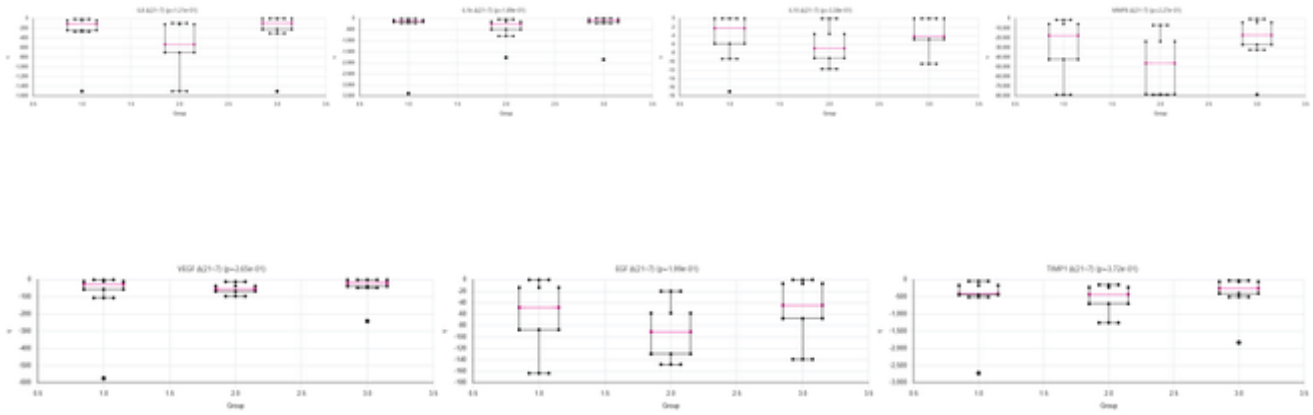

Figure 4. Change score boxplots Δ(Day 21 − Day 7) by group. Rows left→right: IL-8, IL-1β, IL-10, MMP-8 (top); VEGF-A, EGF, TIMP-1 (bottom). X-axis: Group (1=Control, 2=CHX, 3=StellaLife); Y-axis: Change in concentration (pg/mL). All p-values > 0.05.

Correlation Analysis

Spearman correlation analysis revealed strong positive associations among all 21 cytokine-cytokine pairs (Table 5; ρ = 0.788–0.969, p < 0.001). The strongest pair correlations were: IL-8 & IL-1β (ρ = 0.969), EGF & VEGF-A (ρ = 0.962), and MMP-8 & IL-8 (ρ = 0.958). All seven analytes demonstrated significant negative correlations with time (Table 6; ρ = −0.552 to −0.776, all p < 0.001). Figure 5 presents scatter plots of concentration vs. time for all analytes. These findings further support that cytokine expression during palatal wound healing is highly coordinated and primarily driven by temporal progression rather than treatment modality.

Table 5. Spearman correlation matrix — cytokine pairs.

Analyte 1	Analyte 2	Spearman ρ	p-value
IL-8	IL-10	0.802	<0.001
IL-8	EGF	0.930	<0.001
IL-8	VEGF-A	0.904	<0.001
IL-8	MMP-8	0.958	<0.001
IL-8	IL-1β	0.969	<0.001
IL-8	TIMP-1	0.957	<0.001
IL-10	EGF	0.867	<0.001
IL-10	VEGF-A	0.880	<0.001
IL-10	MMP-8	0.829	<0.001
IL-10	IL-1β	0.788	<0.001
IL-10	TIMP-1	0.794	<0.001
EGF	VEGF-A	0.962	<0.001
EGF	MMP-8	0.951	<0.001
EGF	IL-1β	0.927	<0.001
EGF	TIMP-1	0.923	<0.001
VEGF-A	MMP-8	0.914	<0.001
VEGF-A	IL-1β	0.901	<0.001
VEGF-A	TIMP-1	0.885	<0.001
MMP-8	IL-1β	0.945	<0.001
MMP-8	TIMP-1	0.955	<0.001
IL-1β	TIMP-1	0.929	<0.001

Table 6. Spearman correlations of analyte concentrations with time.

Analyte	Spearman ρ (vs. Time)	p-value
IL-8	−0.776	1.13×10^{-17}
IL-1β	−0.773	1.65×10^{-17}
MMP-8	−0.747	7.42×10^{-16}
TIMP-1	−0.708	1.02×10^{-13}
EGF	−0.670	5.74×10^{-12}
VEGF-A	−0.630	2.21×10^{-10}
IL-10	−0.552	7.77×10^{-8}

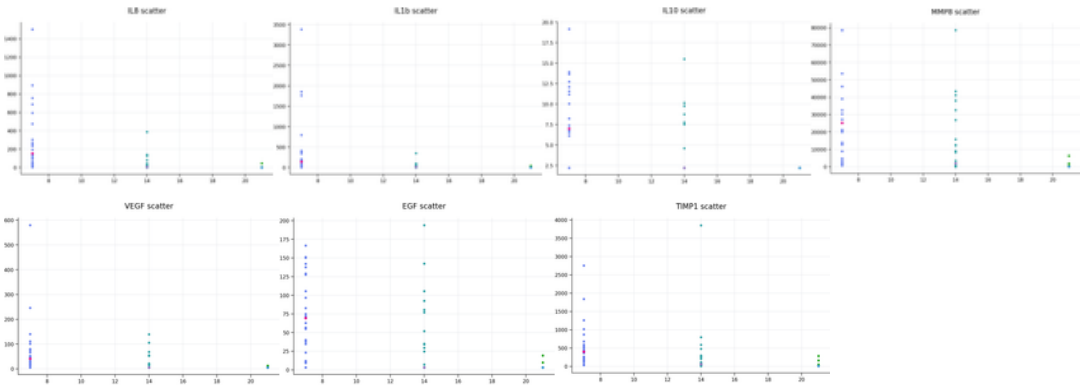

Figure 5. Scatter plots of cytokine concentration vs. time (all groups combined). Rows left→right: IL-8, IL-1β, IL-10, MMP-8 (top); VEGF-A, EGF, TIMP-1 (bottom). X-axis: Day (7, 14, 21); Y-axis: Concentration (pg/mL). Spearman ρ values shown in Table 6.

DISCUSSION

Principal Findings

This study demonstrated two principal findings:
(1) a significant, time-dependent reduction in all seven inflammatory mediators during palatal wound healing following FGG, and
(2) the absence of significant differences among StellaLife, chlorhexidine, and saline groups.
The absence of intergroup differences suggests that the magnitude and coordination of the host inflammatory response following FGG may overshadow subtle pharmacologic or botanical effects. These findings highlight the dominant role of intrinsic wound-healing biology over externally applied adjunctive therapies.

Temporal Cytokine Dynamics

The observed temporal pattern is consistent with the established biological phases of secondary intention wound healing (3,4,14,18,19).
Peak cytokine concentrations at Day 7 correspond to the inflammatory phase, characterized by neutrophil and macrophage activity. Pro-inflammatory mediators such as IL-8 and IL-1β exhibited the steepest decline, reflecting their central role in early inflammation.
MMP-8 and TIMP-1 demonstrated coordinated downregulation, indicating tightly controlled extracellular matrix remodeling during transition to the proliferative phase (15).
The lack of significant differences between Days 14 and 21 suggests that the majority of inflammatory resolution occurs within the first two weeks, consistent with prior studies evaluating cytokine dynamics following periodontal procedures (13,14).

Lack of Treatment Effect

Despite promising in vitro evidence demonstrating anti-inflammatory and cytocompatible properties of StellaLife (6,8,9), these effects were not observed in vivo. One explanation is that the intrinsic biological wound-healing cascade is highly coordinated and may mask subtle treatment-related effects. Additionally, salivary dilution, limited contact time, and mechanical protection from the palatal stent may reduce the effective bioavailability of topical agents. Chlorhexidine's known cytotoxicity in vitro (10,11) does not appear to impair healing clinically, consistent with findings from a recent randomized trial (12). These findings are further supported by clinical studies demonstrating no significant differences in inflammatory markers between herbal formulations and chlorhexidine in vivo (17).

Biological Coordination of Cytokine Networks

Strong positive correlations among cytokines and consistent negative correlations with time indicate that wound healing is governed by a highly coordinated biological network rather than isolated mediator

activity. These findings further support that cytokine expression during palatal wound healing is highly coordinated and primarily driven by temporal progression rather than treatment modality (18–20).

Clinical Implications

Cytokine expression during palatal wound healing appears largely insensitive to adjunctive rinse therapy at the measured time points. While StellaLife may confer benefits in pain control or epithelialization, these effects are unlikely to be mediated through measurable changes in inflammatory cytokine levels.

Limitations

This study has several limitations. The sample size was relatively small, which may limit detection of subtle differences between groups. Cytokine measurements were restricted to three time points, potentially missing early or late events. Additionally, variability in salivary exposure and topical agent retention may have influenced results.

Future Directions

Future studies should integrate cytokine analysis with clinical outcomes and histologic evaluation to better define the relationship between molecular signaling and wound healing. Expanded sampling intervals may further elucidate early inflammatory dynamics.

CONCLUSIONS

Palatal wound healing following free gingival grafting is characterized by a significant, time-dependent reduction in inflammatory cytokines, with peak activity at Day 7 and resolution by Day 21. No significant differences were observed among StellaLife, chlorhexidine, and saline groups, indicating that adjunctive rinses do not meaningfully alter the cytokine profile of the healing wound.

These findings suggest that cytokine dynamics are primarily driven by intrinsic, time-dependent biological processes rather than treatment modality.

REFERENCES

1. Sanz M, Simion M. Surgical techniques on periodontal plastic surgery and soft tissue regeneration. J Clin Periodontol. 2014;41 Suppl 15:S92–7.
2. Tavelli L, Barootchi S, Stefanini M, Zucchelli G, Giannobile WV, Wang HL. Wound healing dynamics, morbidity, and complications of palatal soft-tissue harvesting. Periodontol 2000. 2023;92(1):90–119.
3. Clark RA. Wound repair — overview and general considerations. In: Clark RA, ed. The Molecular and Cellular Biology of Wound Repair. Plenum Press; 1996:3–50.
4. Harper D, Young A, McNaught C-E. The physiology of wound healing. Surgery. 2014;32:445–450.
5. Estrin NE, Romanos GE, Tatch W, Pikos M, Miron RJ. Biological characterization, properties, and clinical use of a novel homeopathic antiseptic oral recovery kit. Oral Health Prev Dent. 2022;20(1):485–499.
6. Fujioka-Kobayashi M, Schaller B, Pikos MA, Sculean A, Miron RJ. Cytotoxicity and gene expression changes of a novel homeopathic antiseptic oral rinse in comparison to chlorhexidine in gingival fibroblasts. Materials (Basel). 2020;13(14):3190.
7. Lee C, Suzuki J. The efficacy of preemptive analgesia using a non-opioid alternative therapy regimen on postoperative analgesia following block bone graft surgery. Clin J Pharmacol Pharmacother. 2019;1(2):1006.
8. Sharma S, Arif M, Nirala RK, et al. Cumulative therapeutic effects of phytochemicals in Arnica montana flower extract alleviated collagen-induced arthritis. J Sci Food Agric. 2016;96(5):1500–10.
9. Zhou P, Chrepa V, Karoussis I, Pikos MA, Kotsakis GA. Cytocompatibility properties of an herbal compound solution support in vitro wound healing. Front Physiol. 2021;12:653661.
10. Mariotti AJ, Rumpf DA. Chlorhexidine-induced changes to human gingival fibroblast collagen and non-collagen protein production. J Periodontol. 1999;70(12):1443–8.
11. Müller HD, Eick S, Moritz A, Lussi A, Gruber R. Cytotoxicity and antimicrobial activity of oral rinses in vitro. Biomed Res Int. 2017;2017:4019723.
12. Pardo C, Sanz M, Herrera D, et al. Early periodontal wound healing after chlorhexidine rinsing: a randomized clinical trial. Clin Oral Investig. 2024;28(6).
13. Yadav VS, Makker K, Tewari N, et al. Expression of wound healing markers in gingival crevicular fluid following root-coverage procedures: a systematic review of randomized clinical trials. Arch Oral Biol. 2024;166:106035.
14. Trombelli L, Farina R, Marzola A, et al. Early healing events after periodontal surgery: observations on soft tissue healing, microcirculation, and wound fluid cytokine levels. Int J Mol Sci. 2017;18(2):283.
15. Keceli HG, Ercan N, Atilla G, et al. Cytokine and MMP levels in gingival crevicular fluid after use of platelet-rich fibrin or connective tissue graft in treatment of gingival recessions. J Periodontal Res. 2015;50(6):761–71.
16. James P, Worthington HV, Parnell C, et al. Chlorhexidine mouthrinse as an adjunctive treatment for gingival health. Cochrane Database Syst Rev. 2017;3:CD008676.
17. Aslam Z, Wu J, Wang Z, Anderson NK, Estrin NE, Romanos GE. Efficacy of herbal vs. chlorhexidine mouthwash in experimental gingivitis: a cross-over clinical and microbiological study. Dent J. 2025;13(12):608.
18. Eming SA, Martin P, Tomic-Canic M. Wound repair and regeneration. Sci Transl Med. 2014;6(265):265sr6.
19. Gurtner GC, Werner S, Barrandon Y, Longaker MT. Wound repair and regeneration. Nature. 2008;453:314–321.
20. Bastian P, Pilloni A, Bloch W, et al. Exudate cytokine profiles during oral wound healing. J Clin Med. 2021;10(12):2626.